HHS Public Access

Author manuscript

J Mol Graph Model. Author manuscript; available in PMC 2018 October 01.

Published in final edited form as:

J Mol Graph Model. 2017 October ; 77: 189–199. doi:10.1016/j.jmgm.2017.08.013.

Understanding Molecular Interactions between Scavenger Receptor A and its Natural Product Inhibitors through Molecular Modeling Studies

Piyusha P. Pagare[a], **Saheem A. Zaidi**[a], **Xiaomei Zhang**[b], **Xia Li**[c,d,e], **Xiaofei Yu**[c,d,e], **Xiang-Yang Wang**[c,d,e], and **Yan Zhang**[a,e,*]

[a]Department of Medicinal Chemistry, School of Pharmacy, Virginia Commonwealth University, 800 East Leigh Street, Richmond, VA 23298, USA

[b]School of Pharmacy, Tianjin Medical University, Tianjin 300070, China

[c]Department of Human and Molecular Genetics, School of Medicine, Virginia Commonwealth University, Richmond, VA 23298, USA

[d]Institute of Molecular Medicine, Virginia Commonwealth University, Richmond, VA 23298, USA

[e]Massey Cancer Center, Virginia Commonwealth University, Richmond, VA 23298, USA

Abstract

Scavenger receptor A (SRA), as an immune regulator, has been shown to play important roles in lipid metabolism, cardiovascular diseases, and pathogen recognition. Several natural product inhibitors of SRA have been studied for their potential application in modulating SRA functions. To understand the binding mode of these inhibitors on SRA, we conducted systematic molecular modeling studies in order to identify putative binding domain(s) that may be responsible for their recognition to the receptor as well as their inhibitory activity. Treatment of SRA with one of the natural product inhibitors, rhein, led to significant dissociation of SRA oligomers to its trimer and dimer forms, which further supported our hypothesis on their putative mechanism of action. Such information is believed to shed light on design of more potent inhibitors for the receptor in order to develop potential therapeutics through immune system modulation.

Graphical Abstract

*Corresponding author. Tel.: +1 804 8280021. yzhang2@vcu.edu (Y. Zhang).

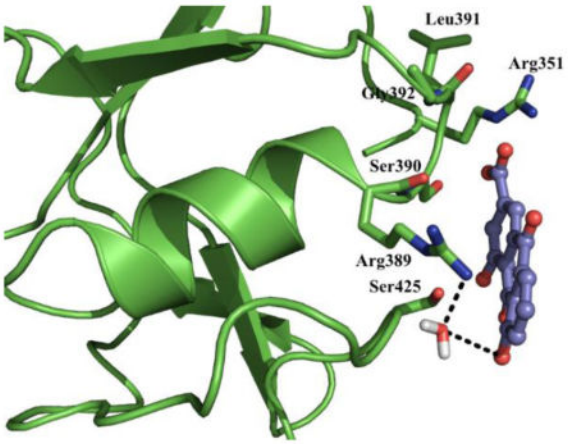

Dimeric SRA model with natural product ligand rhein shown in sticks at the most preferred docking mode.

Keywords

SRA; natural products; inhibitor; docking; molecular dynamics simulation; binding modes

1. Introduction

Scavenger receptor A (SRA) is a newly identified immune regulator and is primarily expressed on myeloid cells, such as macrophages and dendritic cells (DCs).[1] SRA was reported initially as a major receptor on macrophages for internalization of modified lipoproteins.[2,3] Since then, the roles of SRA in lipid metabolism, cardiovascular diseases (e.g. atherosclerosis), and pathogen recognition have been well documented.[4–8] Our previous work revealed a novel feature of SRA action in attenuating antigen-specific T cell responses, and impeding therapeutically induced antitumor immunity generated by cancer vaccines.[3,9–14] The immunoregulatory effect of SRA in these contexts has been attributed, at least in part, to the reduced immunostimulatory capacity of antigen-presenting cells (APCs), e.g., DCs, in priming tumor antigen-specific T cells. Our molecular studies demonstrated that disruption of the TLR4-NF-κB signaling cascades in DCs by SRA reduced the expression of co-stimulatory molecules (CD80, CD86) and production of inflammatory cytokines/chemokines (IL-12, IFN-β, IP10).[10,15] Therefore, targeting SRA may provide a novel approach to enhance antitumor immunity.

Many of the ligands for SRA are polyanionic. Interestingly, a number of natural products have been reported as potential SRA inhibitors with varied biological activities.[16,17] Among them, sennoside B and tannic acid were able to reduce SRA mediated antigen transfer.[17] Particularly, sennoside B was shown to be able to reduce T cell proliferation both in vitro and in vivo. However, the high molecular weight (>1,000) of most of these compounds makes them not suitable for further drug development. Our recent effort in identifying small molecule SRA inhibitors showed promise in reducing the size of the molecule while maintaining the desired pharmacological properties.[18,19] For example, natural products like

rhein, the deconstruction product of sennoside B and danthron, the deconstruction analog of rhein, partially reversed the suppressive activity of SRA in DC-primed T cell activation and suppressed the SRA ligand poly (I:C) triggered signaling. All these results indicate that development of small molecule inhibitor for SRA would be a valid route for intervention of diseases by targeting SRA-associated activity. To further understand the interaction between small molecule inhibitors and their target protein SRA, we herein report the molecular modeling studies of these natural products en route to understand their possible mechanism of action.

2. Results and discussion

2.1. Structural comparison and conformation analysis of the inhibitors

The chemical structures of four natural product inhibitors are shown in Figure 1. The common structural feature in them is the phenolic moiety. While Tannic acid is primarily a polyphenol molecule, sennoside B, rhein and danthron also contain phenolic groups with additional presence of carboxylic group in sennoside B and rhein making them more acidic than tannic acid. Glucose unit exists in both tannic acid and sennoside B, while for tannic acid its glucose is the core unit and for sennoside B two glucoses are at the branching out sections.

To obtain a reasonable starting point for further study of these natural products, their lowest energy conformation was obtained first (Fig. 2). The conformation of tannic acid was very flexible while overall it appeared to prefer an extended planar one. The two chiral centers in sennoside B made the whole molecule somewhat a staggered conformation while the anthracenic structure made rhein and danthron completely planar conformations.

2.2 SRA homology model construction

SRA belongs to the class A scavenger receptor family and it is composed of six structural domains: N-terminal cytoplasmic, transmembrane, spacer, α helical coiled coil, collagenous, and cysteine rich (Fig. 3). Regarding to its possible ligand domain(s), it is still a matter of investigation. For example, its collagenous domain has been implicated in binding for denatured and native collagens and modified lipoproteins.[18] Recently the cysteine rich domain of SRA was shown to also serve as a potential binding site for Ac-LDL.[20] We recently completed the construction of SRA cysteine rich domain homology models[18] based on the available crystal structures of the cysteine rich domain of MARCO, another member of class A scavenger receptor family, in its monomeric and dimeric form (PDB: 2OY3 and 2OYA).[21] Mouse scavenger receptor MARCO had the highest sequence identity (43%) and homology (63%) to SRA and the fact that both proteins belong to the same receptor family, made the crystal structure of MARCO a suitable choice as the template for homology modeling. The homology models were built using MODELLER v10.2 and the local geometry of the optimized structure was checked using PROTABLE and PROCHECK (Supplementary Information). Primarily, the putative binding sites for rhein were first identified through exhaustive ligand docking on the built homology models using GOLD5.4[22] followed by HINT[23] (Hydropathic INTeractions) scoring.[18]

2.3 Docking of tannic acid, sennoside B, and danthron on SRA monomer model

The docking strategy employed for tannic acid, sennoside B and danthron was similar to that employed earlier for rhein, as reported previously.[18] Based on the hydrophobic and electrostatic properties of the protein surface, five unique binding sites were observed on SRA monomer model. The obtained HINT scores are summarized in Table 1, 2 and 3. In our practice, we noticed that sometimes the best HINT score from certain docking process could be an outlier if considering some special docking pose between the ligand and its target protein. On the other hand, the average HINT score may provide equal weightage to each docked solution despite that most of the solutions are likely to be sub-optimal. Meanwhile Boltzmann distribution analysis was also adopted in our practice based on the fact that it weights the data with reference to the best score and thus provides more weightage to the optimal solutions.

Combining all three scoring functions, it seemed that tannic acid showed no significant preference to any one site on the monomer, sennoside B preferred site **2** (which is a similar site for rhein for its monomer binding site) while danthron showed preference for site **3** on the monomer model of SRA (Table 1, 2 and 3). Figure 4 illustrates the best Boltzmann average HINT scored-docking poses of tannic acid on all four sites, Figure 5 of sennoside B on binding site **2** and Figure 6 of danthron on **3**.

In the rhein's preferred binding pose on the monomer model, a cluster of the basic residues (Arg382, 389, 422 and Gln385) formed the primary binding locus. While for danthron three of these basic residues (Gln385, Arg389 and Arg422) participated in the binding locus; for sennoside B, only two of these residues (Arg382 and Gln385) participated in the binding locus (Table 4). Several hydrophobic residues were observed to interact with the backbone of the molecule more significantly. For tannic acid, due to its much larger molecular size compared to rhein, danthron and sennoside B, more residues from the protein got involved into the interaction with the ligand. All four "preferred" sites seemed to contribute equally to the recognition of the ligand to the protein. Only site **3** seemed to share several same residues with the sites for rhein and sennoside B.

The ambiguity of such an observation among all three ligands (along with rhein) of their binding mode on the target protein suggests that the monomer model of SRA might not be the most suitable to predict potential ligand interaction with the SRA cysteine rich domain. Certainly, it does not exclude the possible effect from the conformation flexibility of tannic acid.

2.4. Docking of tannic acid and sennoside B on SRA dimer model

Previously, based on the hydrophobic and electrostatic properties of the SRA dimer model surface, besides the binding sites on the monomer, four additional binding sites were observed by focusing mainly on the interface of the two monomers for rhein.[18] As one of the binding sites displayed the highest HINT scores in all three scoring categories, it was postulated as the plausible binding site for rhein to interact with the SRA cysteine rich domain. Particularly Ile365, 426, and 431 of one subunit formed a hydrophobic cavity to interact with the anthraquinone backbone of rhein in addition to Arg351 (from the other

monomer subunit, therefore, the interface), Ser390, and Ser425 side chains acted as hydrogen bond donors while Leu366 backbone carbonyl and Glu427 side chain served as hydrogen bond acceptors. Docking of danthron in this putative binding site also resulted in very similar binding interactions particularly with the residues Ile365, Leu366, Ser390, and Ser425.[19]

Very interestingly, from the docking studies of both tannic acid and sennoside B, one particular binding site displayed the highest HINT scores in all three scoring categories among four optional sites (Table 1 and 2). Looking at the amino acid residues that were involved in the interaction with the ligands, a surprising majority of them came from the same group that was also observed to be interacting with rhein and danthron for their highest scored binding pose (Table 4). These residues provided potential hydrogen bonding and hydrophobic force to stabilize the ligand at the shallow surface of the protein. For tannic acid, the only unique feature came from Glu428, which might interact with one of the hydroxyl phenol group through hydrogen bonding. The rest of its binding pocket looked exactly the same as the one for sennoside B.

Figures 7 and 8 illustrate the best Boltzmann average HINT scored-docking pose of tannic acid and sennoside B on the SRA dimer domain respectively. In addition to the common features, for sennoside B, His367 and Trp434 seemed to provide aromatic stacking interaction with the backbone of the small molecule; while Val350, on the other hand, joined Ile365 and Ile426 to reinforce the hydrophobic interaction with the ligand.

To further compare the binding mode of all four natural products in the putative dimer binding pocket, the electrostatic potential analysis of the dimer was conducted (Fig. 9). The electrostatic potential map of the monomer model shows a relatively electronegative surface (Fig. S3). It appears that due to the interaction between two monomers units, the predicted binding site on the dimer becomes more electropositive (characterized by a relative absence of electrons) as compared to rest of the protein. Thus, this site would serve as an ideal site for molecules with higher electronegativity. All four natural products, i.e. tannic acid, sennoside B, rhein, and danthron being polyanionic would thus interact favorably at this predicted ligand binding site of the dimer over the monomer binding sites.

2.5 Molecular dynamics simulations of tannic acid, sennoside B, rhein and danthron with SRA dimer homology model

To further understand the binding modes of tannic acid, sennoside B, rhein, and danthron with the SRA dimer, we performed molecular dynamics (MD) simulations on these complexes based on their optimal docking modes. For obtaining stable systems, 10 ns MD simulations on the protein homology model as well as the four complexes were carried out. For each complex, the system was enclosed in a water box of dimension 96 Å × 96 Å × 96 Å and appropriate number of Cl^- and Na^+ ions to make up the concentration to 50mM were added to neutralize the system. After that, the root-mean-square deviation (RMSD) values of all the protein backbone atoms were calculated to ensure the stability of all the systems.

Due to the highly flexible nature of the protein as well as the natural product tannic acid, higher RMSD values were obtained for protein-tannic acid complex. Protein complex with

rhein and danthron also seem to show higher RMSD values which can again be attributed to the highly flexible nature of the protein. Danthron, especially, due to loss of the carboxyl group in its structure, becomes a relatively hydrophobic molecule as compared to other three natural products. Due to the electropositive nature of the binding site, the RMSD values for the protein-danthron complex might be higher. Sennoside B, although a large and flexible molecule, showed RMSD values in the accepted range. One reason for this might be that water molecules seem to be involved in stabilizing the protein-sennoside B complex (Fig. 11). Comparing the RMSD values of the backbone atoms in all systems after 5 ns and 8 ns minimum change was observed (SRA 0.15Å, SRA-tannic acid 1.6Å, SRA-sennoside B 0.2Å, SRA-rhein 1.2Å, and SRA-danthron 0.44Å) (Figure 10) thus after 5ns equilibration process, the average RMSD values obtained for these complexes seem to be in an accepted range, indicating the complexes reached to a relatively stable status.

Following this, interactions of tannic acid, sennoside B, rhein, and danthron with the SRA-dimer model were analyzed for the MD trajectory and the results were summarized in Table 5. Although the overall binding pocket remained the same, there were some differences observed in the interacting residues after MD simulation (Fig. 11). For example, amino acid residues Arg351, Ile365, Leu366, Ser390 and Ser425 still appeared to be critical for binding of these natural products as seen from docking results. Due to the large size and polyionic nature of tannic acid, additional residues were observed contributing hydrogen-bonding to stable this ligand-protein complex. Simulation of sennoside B-SRA complex did not affect its binding. Despite the large size of sennoside B, it allowed for two water mediated interactions with the protein residue Arg351. These water mediated hydrogen bonding interactions might be responsible for locking the conformation of the flexible natural product and establish its interaction with Arg351. Although rhein showed similar interactions with the protein before and after MD simulations, Glu427 which showed hydrogen bonding interactions with one of the hydroxyl groups from the docking results did not appear to be critical after the simulation. On the other hand, Arg389 appeared to be an important residue forming water mediated hydrogen bonding interactions with the hydroxyl group of the molecule. Interestingly, danthron showed hydrophobic interactions with residues Val350, Val363, Ile365, Leu366, Trp373, Val387 and Ile426 and π-π interactions with Trp373, thus making the binding pocket vey hydrophobic. Ser390, Ser424 and Ser425 appeared to be involved in hydrogen bonding interactions with danthron. Water mediated hydrogen bonding, similar to rhein, was also seen between Ser425 and danthron.

Based on the above analysis it is not difficult to see that docking studies of four natural product inhibitors on SRA dimer model seemed to provide a more unified result compared to the studies on the monomer one. In addition to the collagenous domain of SRA I and II, which has been implicated in binding to a number of ligands including denatured type I, III collagen, native type IV collagen, and modified lipoproteins (e.g. AcLDL), their scavenger receptor cysteine rich (SRCR) domain was also reported to be a functional binding domain for AcLDL under certain physiological conditions. In comparison, MARCO has also been reported to require the SRCR domain for ligand binding. As a matter of fact, it has been postulated that the two trimeric MARCO molecules might dimerize through their SRCR domains by a domain-swapping mechanism.[21] Such an assembly could then proceed to form oligomers to provide a large surface capable of interacting with large ligands, such as

modified LDL. The dimer's crystal structure of the MARCO SRCR domain seemed to support such a hypothesis.

In comparison, the active forms of both type I and type II SRA are trimeric integral transmembrane glycoproteins (220 kDa), which can bind a wide variety of polyanions, are composed of disulfide-lined dimers (150 kDa) and noncovalently associated monomers (77 kDa).[2,24–28] Under physiological conditions, SRA also exists in multimeric forms. Our dimeric homology model of SRA I SRCR domain was constructed based on the dimerized MARCO SRCR domain crystal structure, therefore, it is logic to hypothesize that the binding of rhein and possibly other natural product inhibitors on the dimeric interface of SRA I SRCR domain would interfere the oligomerization of SRCR domains of SRA, then further inhibit the binding of endogenous ligands, and modulate the function of SRA. To test this hypothesis primarily, we incubated SRA-Fc fusion proteins secreted from a 293T-SRA stable cell line with different doses of rhein at 37°C for 2 hours, and then subjected to analysis using 4–16% native PAGE gel. Figure 13 showed that after rhein treatment, there was a significant increase of trimers and dimers when compared with control group, which mainly contained oligomer. However, no significant dose-dependent increase in the forms of dimers or trimers was observed, suggesting that 100 μM rhein may have a full effect with the amount of protein incubated. These observations further defined the role of rhein as a potential lead to design and develop novel inhibitors of SRA to modulate its immune functions.

3. Conclusion

To gain insights into the interaction between natural product inhibitors and SRA at a molecular level, as well as to guide future molecular design of small molecule SRA inhibitors, a systematic and progressive molecular modeling study was conducted for four natural product SRA inhibitors on the monomer and dimer homology models of SRA. The results indicated that the dimer model provided more consistent information regarding to the binding pocket composition and ligand binding mode. Experimental evidence came from our observation that treatment with rhein can partially dissociate or antagonize the oligomerization of SRA, resulting in increased formation of trimers and dimers. Among all the natural product inhibitors, it seems to us that rhein and danthron would act as reasonable leads for further modification to achieve more potent inhibitors for the protein. Information obtained here will be helpful for future effort to construct more complex and complimentary 3D structure of the protein, particularly the cysteine rich domain, as well as to design more potent small molecule inhibitor to modulate SRA function for potential therapeutic applications.

4. Materials and methods

4.1. Conformation analysis of small molecule inhibitors

The molecular structures of tannic acid, sennoside B, rhein and danthron were sketched in SYBYL-X 2.1.1, and Gasteiger–H ckel charges were assigned before energy minimization (10,000 iterations) with the Tripos force field (TFF). The molecules were then solvated with a corresponding water box. Next, energy minimizations were performed with initial

temperature at 300K and periodic boundary conditions with a 2 fs time-step. The energy-minimized average for the 10,000 fs of simulation for all 3 ligands was depicted. Figures were generated using the PyMOL Molecular Graphics system, Version 1.7.4.

4.2. Sequence analysis and model construction

In order to identify a suitable template for homology modeling operation of SRA, database search was performed using the basic local alignment search tool (BLAST). From these results, mouse scavenger receptor MARCO had the highest sequence identity (43%) and homology (63%) to SRA. Also the fact that both, SRA and MARCO, belong to the same receptor family, makes crystal structure of MARCO a viable choice as the template for homology modeling. One of the most important steps in homology modeling study is the sequence alignment between the target and the template amino acid sequence. The sequence alignment between SRA and MARCO was performed using the program ClustalX 2.0.12[29] (Supplementary Information).

The homology models were built for both the monomeric and dimeric forms of human SRA protein using X-ray crystal structures of monomeric (PDB ID – 2OY3)[21] and dimeric mouse scavenger receptor MARCO (PDB ID – 2OYA)[21] respectively, as the templates using MODELLER v10.2.[30] The local geometry of the optimized structure was checked using PROTABLE and PROCHECK. PROTABLE results showed that all amino acid residues had reasonable bond lengths and bond angles. The Ramachandran plot obtained from PROCHECK was shown in Supplementary Information. As seen from the Ramachandran plot, nearly 94% of the amino acid residues were either in the most favored regions or the additionally allowed regions.

The homology models were then utilized for ligand docking using GOLD5.4[22] under default settings at different sites of the protein models. The generated ligand-receptor models were then exhaustively minimized under Tripos force field in SybylX2.1.1 in order to remove clashes and minimize strain energy, so as to optimize interactions between ligand and the protein. Thus, obtained models were subjected to further hydropathic interaction analyses using HINT[23] program. The figures shown were generated using PyMOL Version 1.7.4.

4.3. Docking studies

Using GOLD 5.4, rhein was docked into different sites of both the monomer and dimer models. The putative binding area was restricted to a 10Å radius around Ile426, Gln385, Phe418, Lys401 and Va353 corresponding to the five monomer sites as well as Ser425, Leu391, Ile365 and Glu361 corresponding to the four sites in the dimer. Tannic acid, sennoside B, rhein and danthron were docked into the models with a total of 100 iterations. This docking of ligands was followed by energy minimization under Tripos force field in SybylX2.1.1 to optimize the structural models for the ligand–protein complexes. CHEMPLP and GOLD scores, which have been optimized for modeling steric complementarity between ligand and protein along with distance- and angle-dependent hydrogen bonding, were used to obtain plausible docking poses. The obtained poses were then rescored with HINT (Hydropathic INTeractions), an empirical free energy scoring tool based on the experimental measurements of log *P* for 1-octanol and water, to estimate atomic level free energies

associated with noncovalent interactions. Optimal docking poses for each ligand–receptor complex were chosen by the highest GOLD and HINT scores. The figures shown were generated using PyMOL Version 1.7.4.

4.4 Molecular dynamics simulations

The homology models of the protein and its complexes with tannic acid, sennoside B, rhein, and danthron were refined by subjecting them to an all-atom Molecular Dynamics (MD) simulation. MD simulations were carried out with the NAMD 2.9 package developed by the Theoretical and Computational Biophysics Group in the Beckman Institute for Advanced Science and Technology at the University of Illinois at Urbana-Champaign.[31] CHARMM (Charmm-27) was used as the force field.[32] The 3D-homology models of the SRA-dimer and its complexes with tannic acid, sennoside B, rhein and danthron were first solvated in an equilibrated TIP3P water box of dimension 96 Å × 96 Å × 96 Å using the center of mass of the complex as the origin. Then Cl^- and Na^+ ions were added to neutralize the system and appropriate number of ions were added up to a concentration of 50 mM. Solvent molecules were first minimized for 500 steps of conjugate gradients minimization method, keeping the protein molecules fixed to allow favorable distribution of water molecules on the complex surface. Subsequently, the system was coupled to a heat bath from 0 to 300 K and the constraints applied to the solute atoms were gradually decreased after which, the system was allowed to be simulated without restraints for over a period of 10 ps. Finally, a 10 ns molecular dynamics production phase was carried out on the entire systems. The analysis of the MD trajectory was done in VMD.[33] All figures were generated using PyMOL Version 1.7.4.

4.3. Generation of SRA-Fc fusion protein

The mouse IgG2aFc portion was fused to the N-terminus of the mouse SRA extracellular domain (residues 79-458), and cloned into a modified pcDNA3.1 vector (Invitrogen). The Fc region comprises the CH2 and CH3 domains of the IgG heavy chain and the hinge region. The amino acids that are critical for FcγRs and C1q binding were mutated to minimize the cytotoxicity and FcR-mediated binding. For constitutive overexpression of the fusion protein, 293T cells were stably transfected with the construct. Western blotting of 293T-SRA stable cell supernatant with anti-mouse SRA antibody (R&D systems) confirmed the secretion of the fusion protein.

4.5. Cell culture and native PAGE electrophoresis

293T-SRA stable cells were cultured in DMEM (Hyclone, Logan, UT, USA) supplemented with 10% fetal bovine serum (FBS), 100 U/ml penicillin and 100 mg/ml streptomycin at 37°C in a humidified incubator containing 5% CO2. 5×10^5 293T-SRA cells were seeded in 24-well plate for 24hr. After the cell reached 80% confluency, medium were removed, cells were washed with PBS once, and then serum-free DMEM were added in each well. After 24h incubation, supernatant were collected, and cell debris were removed. 50 μl supernatant was incubated with or without different doses of rhein at 37°C for 2 hrs. The samples were then subjected to 4–16% native PAGE gel electrophoresis, and western blotting were performed with anti-mouse SRA antibodies.

Acknowledgments

The research was partially supported by Virginia Commonwealth University Massey Cancer Center Pilot Project Grant and by National Institutes of Health (NIH) Grant DA024022, DA044855, CA175033 and CA154708.

References

1. Platt N, Haworth R, Darley L, Gordon S. The many roles of the class A macrophage scavenger receptor. International Review of Cytology. 2002; 212:1–40. [PubMed: 11804035]
2. Kodama T, Reddy P, Kishimoto C, Krieger M. Purification and characterization of a bovine acetyl low density lipoprotein receptor. Proceedings of the National Academy of Sciences of the United States of America. 1988; 85:9238–9242. [PubMed: 3194423]
3. Freeman M, Ashkenes J, Rees DJ, Kingsley DM, Copeland NG, Jenkins NA, Krieger M. An ancient, highly conserved family of cysteine-rich protein domains revealed by cloning type I and type II murine macrophage scavenger receptors. Proceedings of the National Academy of Sciences of the United States of America. 1990; 87:8810–8814. [PubMed: 1978939]
4. Suzuki H, Kurihara Y, Takeya M, Kamada N, Kataoka M, Jishage K, Ueda O, Sakaguchi H, Higashi T, Suzuki T, Takashima Y, Kawabe Y, Cynshi O, Wada Y, Honda M, Kurihara H, Aburatani H, Doi T, Matsumoto A, Azuma S, et al. A role of macrophage scavenger receptors in atherosclerosis and susceptibility to infection. Nature. 1997; 386:292–296. [PubMed: 9069289]
5. Ricci R, Sumara G, Sumara I, Rozenberg I, Kurrer M, Akhmedov A, Hersberger M, Eriksson U, Eberli FR, Becher B, Boren J, Chen M, Cybulsky MI, Moore KJ, Freeman MW, Wagner EF, Matter CM, Luscher TF. Requirement of JNK2 for scavenger receptor A-mediated foam cell formation in atherogenesis. Science. 2004; 306:1558–1561. [PubMed: 15567863]
6. Peiser L, De Winther MP, Makepeace K, Hollinshead M, Coull P, Plested J, Kodama T, Moxon ER, Gordon S. The class A macrophage scavenger receptor is a major pattern recognition receptor for Nesseria meningitidis which is independent of lipopolysaccharide and not required for secretory responses. Infection and Immunity. 2002; 70:5346–5354. [PubMed: 12228258]
7. Stephen SL, Freestone K, Twigg MW, Homer-Vanniasinkam S, Walker JH, Wheatcroft SB, Ponnambalam S. Scavenger receptors and their potential as therapeutic targets in the treatment of cardiovascular disease. International Journal of Hypertension. 2010; 2010:646929. [PubMed: 20981357]
8. Kzhyshkowska J, Neyen C, Gordon S. Role of macrophage scavenger receptos in atherosclerosis. Immunobiology. 2012; 217:492–502. [PubMed: 22437077]
9. Wang XY, Facciponte J, Chen X, Subjeck JR, Repasky EA. Scavenger receptor-A negatively regulates antitumor immunity. Cancer Research. 2007; 67:4996–5002. [PubMed: 17510431]
10. Yi H, Yu X, Gao P, Wang Y, Baek SH, Chen X, Kim HL, Subjeck JR, Wang XY. Pattern recognition scavenger receptor SRA/CD2014 down-regulates Toll-like receptor 4 signaling-dependent CD8 T-cell activation. Blood. 2009; 113:5819–5828. [PubMed: 19349620]
11. Qian J, Yi H, Guo C, Yu X, Zuo D, Chen X 3rd, Kane JM, Repasky EA, Subjeck JR, Wang XY. CD204 suppresses large heat shock protein-facilitated priming of tumor antigen gp100-specific T cells and chaperone vaccine activity against mouse melanoma. Journal of Immunology. 2011; 187:2905–2914.
12. Guo C, Yi H, Yu X, Hu F, Zuo D, Subjeck JR, Wang XY. Absence of scavenger receptor A promotes dendritic cell-mediated cross-penetration of cell-associated antigen and antitumor immune response. Immunology and Cell Biology. 2012; 90:101–108. [PubMed: 21383767]
13. Yi H, Guo C, Yu X, Gao P, Qian J, Zuo D, Manjili MH, Fisher PB, Subjeck JR, Wang XY. Targeting the immunoregulatory SRA/CD204 potentiates specific dendritic cell vaccine-induced T-cell response and antitumor immunity. Cancer Research. 2011; 71:6611–6620. [PubMed: 21914786]
14. Guo C, Yi H, Yu X, Zuo D, Qian J, Yang G, Foster BA, Subjeck JR, Sun X, Mikkelsen RB, Fisher PB, Wang XY. In situ vaccination with CD204 gene-silenced dendritic cell, not unmodified dendritic cell, enhances radiation therapy of prostate cancer. Molecular Cancer Therapeutics. 2012; 11:2331–2341. [PubMed: 22896667]

15. Yu X, Guo C, Zuo D, Wang Y, Kim HL, Subjeck JR, Wang XY. Pattern recognition scavenger receptor CD204 attenuates Toll-like receptor 4-induced NF-kappaB activation by directly inhibiting ubiquitination of tumor necrosis factor (TNF) receptor-associated factor 6. The Journal of Biological Chemistry. 2011; 286:18795–18806. [PubMed: 21460221]
16. Herber DL, Cao W, Nefedova Y, Novitskiy SV, Nagaraj S, Tyurin VA, Corzo A, Cho HI, Celis E, Lennox B, Knight SC, Padhya T, McCaffrey TV, McCaffrey JC, Antonia S, Fishman M, Ferris RL, Kagan VE, Gabrilovich DI. Lipid accumulation and dendritic cell dysfunction in cancer. Nature Medicine. 2010; 16:880–886.
17. Raycroft MT, Harvey BP, Bruck MJ, Mamula MJ. Inhibition of antigen trafficking through scavenger receptor A. The Journal of Biological Chemistry. 2012; 287:5310–5316. [PubMed: 22215667]
18. Yuan Y, Li X, Zaidi SA, Arnatt CK, Yu K, Guo C, Wang XY, Zhang Y. Small molecule inhibits activity of scavenger receptor A: Lead identification and preliminary studies. Bioorganic and Medicinal Chemistry Letters. 2015; 25:3179–3183. [PubMed: 26094120]
19. Zheng Y, Pagare PP, Yuan Y, Wang XY, Zhang Y. Design, synthesis and characterization of rhein analogs as novel inhibitors of scavenger receptor A. Bioorganic and Medicinal Chemistry Letters. 2017; 27:72–76. [PubMed: 27884693]
20. Huang FL, Shiao YJ, Hou SJ, Yang CN, Chen YJ, Lin CH, Shie FS, Tsay HJ. Cysteine-rich domain of scavenger receptor AI modulates the efficacy of surface targeting and mediates oligomeric Abeta internalization. Journal of Biomedical Science. 2013; 20:54. [PubMed: 23915271]
21. Ojala JR, Pillarainen T, Tuuttila A, Sandalova T, Tryggvason K. Crystal structure of the cysteine-rich domain of scavenger receptor MARCO reveals the presence of a basic and acidic cluster that both contribute to ligand recognition. The Journal of Biological Chemistry. 2007; 282:16654–16666. [PubMed: 17405873]
22. Jones G, Willett P, Glen RC, Leach AR, Taylor R. Development and validation of a genetic algorithm for flexible docking. Journal of Molecular Biology. 1997; 267:727–748. [PubMed: 9126849]
23. Sarkar A, Kellogg GE. Hydrophobicity-shake flasks, protein folding and drug discovery. Current Topics in Medicinal Chemistry. 2010; 10:67–83. [PubMed: 19929828]
24. Goldstein JL, Basu SK, Brown MS. Receptor-mediated endocytosis of low-density lipoprotein in cultured cells. Methods in Enzymology. 1983; 98:241–260. [PubMed: 6321901]
25. Goldstein JL, Ho YK, Basu SK, Brown MS. Binding site on macrophages that mediates uptake and degradation of acetylated low density lipoprotein, producing massive cholesterol deposition. Proceedings of the National Academy of Sciences of the Unites States of America. 1979; 76:333–337.
26. Kodama T, Freeman M, Rohrer L, Zabrecky J, Matsudaira P, Krieger M. Type I macrophage scavenger receptor contains alpha-helical and collagen-like coiled coils. Nature. 1990; 343:531–535. [PubMed: 2300204]
27. Rohrer L, Freeman M, Kodama T, Penman M, Krieger M. Coiled-coil fibrous domains mediate ligand binding by macrophage scavenger receptor type II. Nature. 1990; 343:570–572. [PubMed: 2300208]
28. Penman M, Lux A, Freedman NJ, Rohrer L, Ekkel Y, McKinstry H, Resnick D, Krieger M. The type I and type II bovine scavenger receptors expressed in Chinese hamster ovary cells are trimeric proteins with collagenous triple helical domains comprising noncovalently associated monomers and Cys83-disulfide-linked dimers. The Journal of Biological Chemistry. 1991; 266:23985–23993. [PubMed: 1748671]
29. Larkin MA, Blackshields G, Brow NP, Chenna R, McGettigan PA, McWilliam H, Valentin F, Wallace IM, Wilm A, Lopez R, Thompson JD, Gibson TJ, Higgins DG. Clustal W and Clustal X version 2.0. Bioinformatics. 2007; 23:2947–2948. [PubMed: 17846036]
30. Sali A, Blunder TL. Comparative protein modeling by satisfaction of spatial restraints. Journal of Molecular Biology. 1993; 234:779–815. [PubMed: 8254673]

31. Phillips JC, Braun R, Wang W, Gumbart J, Tajkhorshid E, Villa E, Chipot C, Skeel RD, Kale L, Schulten K. Scalable molecular dynamics with NAMD. Journal of Computational Chemistry. 2005; 26:1781–1802. [PubMed: 16222654]

32. MacKerell AD Jr, Bashford D, Bellott M, Dunbrack RL Jr, Evanseck JD, Field MJ, Fischer S, Gao J, Gao H, Ha S, Joseph-McCarthy D, Kuchnir L, Kuczera K, Lau FTK, Mattos C, Michnick S, Smith JC, Stote R, Starub J, Watanabe M, Wiorkiewicz-Kuczera J, Yin D, Karplus M. All-atom empirical potential for molecular modeling and dynamics studies of proteins. Journal of Physical Chemistry. 1998; 102:3586–3616. [PubMed: 24889800]

33. Humphrey W, Dalke A, Schulten K. VMD-Visual Molecular Dynamics. Journal of Molecular Graphics. 1996; 14:33–38. [PubMed: 8744570]

Highlights

- To gain insights into the interaction between natural product inhibitors and SRA at molecular level, we constructed monomer and dimer homology models of SRA.
- To understand the binding mode of these inhibitors, we conducted docking study andmolecular dynamics simulations, identified putative binding domain(s) that may beresponsible for their recognition to the receptor as well as their inhibitory activity.
- The results indicated that the dimer model provided more consistent information regarding to the binding pocket composition and ligand binding mode.
- Treatment of SRA with rhein led to significant dissociation of SRA oligomers to its trimer and dimer form supporting our hypothesis of their putative mechanism of action.
- Such information will be helpful in designing more potent small molecule inhibitor to modulate SRA function for potential therapeutic application.

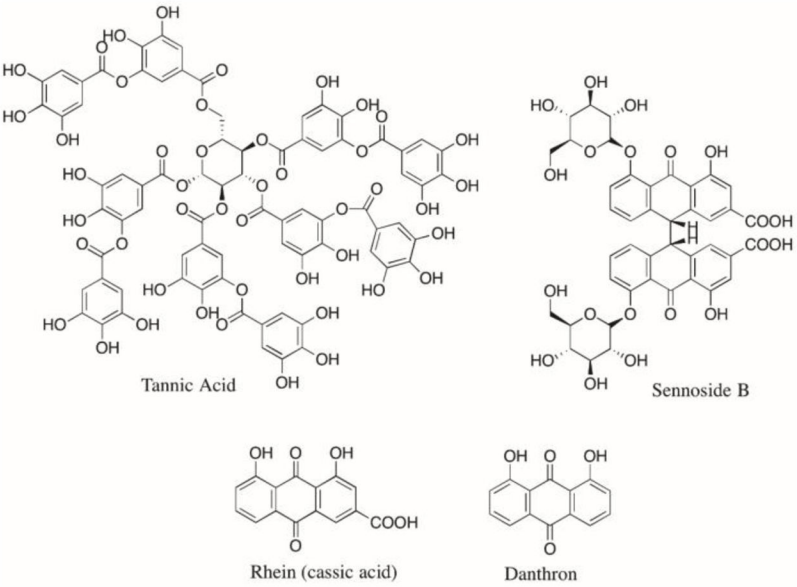

Fig. 1.
Chemical structures of natural product SRA inhibitors.

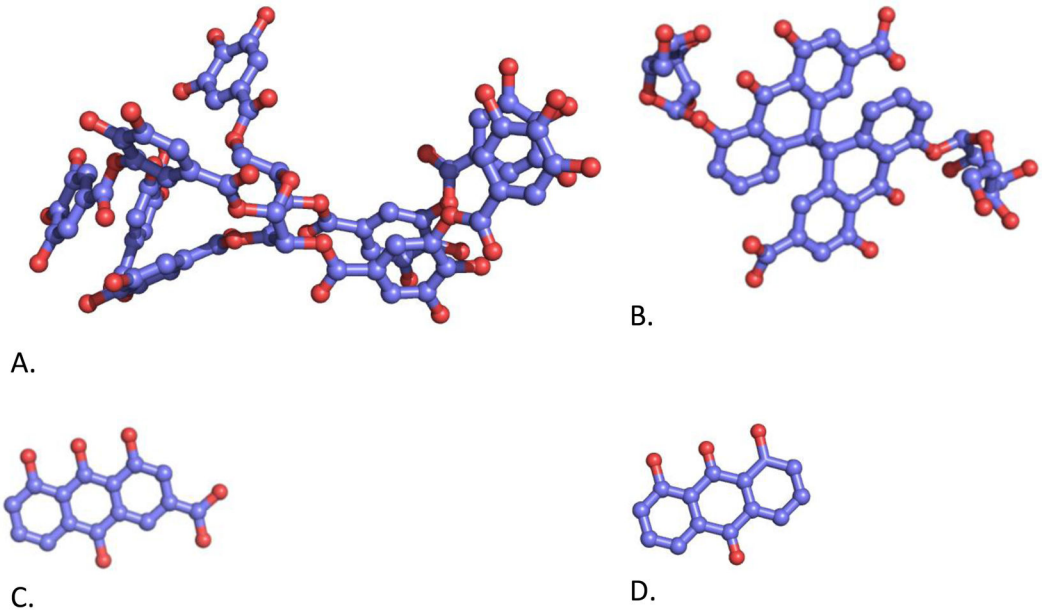

Fig. 2.

Lowest energy conformation of four natural product SRA inhibitors. A) Tannic acid; B) Sennoside B; C) Rhein; and D) Danthron.

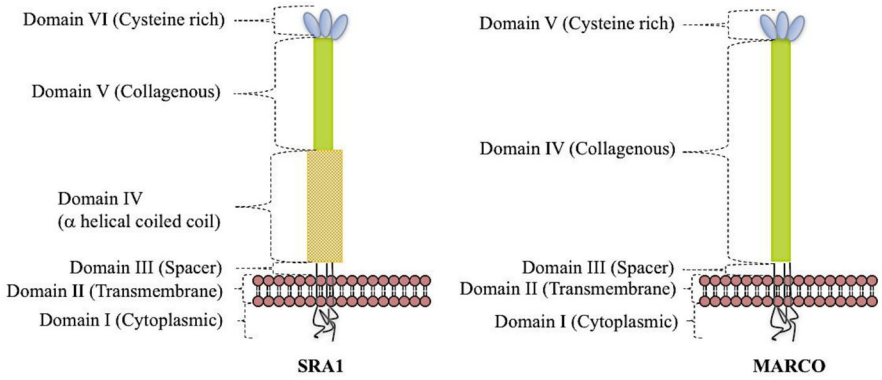

Fig. 3.
Schematic of the structural domains of Scavenger Receptor A and MARCO.

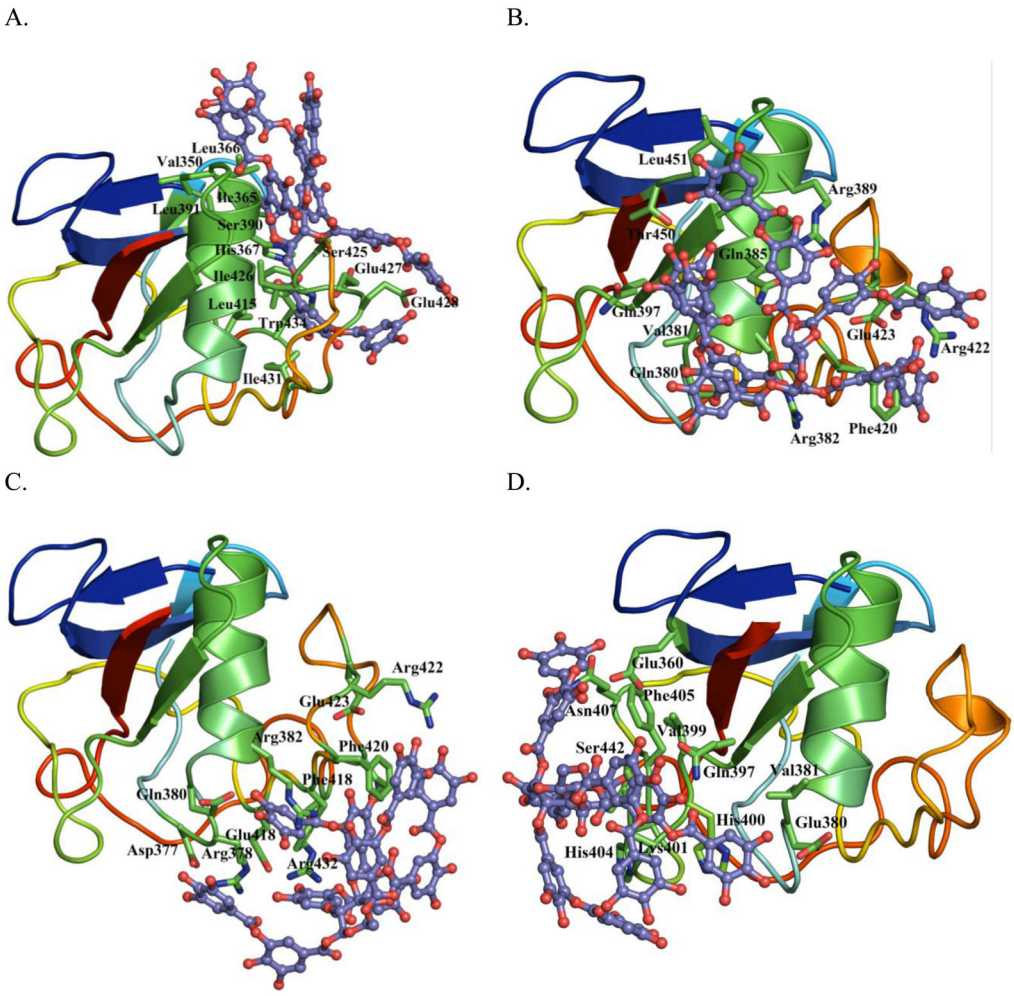

Fig. 4.

Docking modes of tannic acid (in balls and sticks) on SRA domain monomer (cartoon representation). Amino acid residues involved in putative interactions are shown in green sticks representation: A) Site 1; B) Site 2; C) Site 3; D) Site 4.

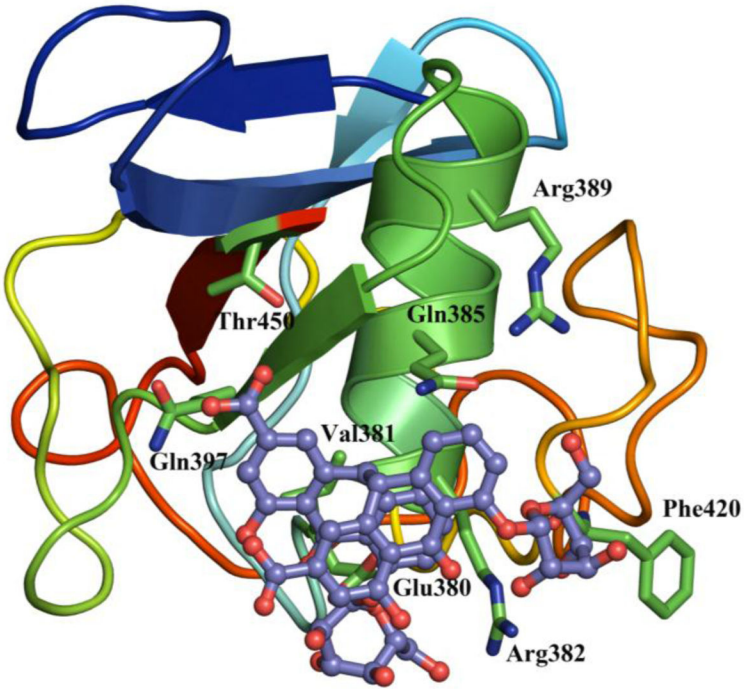

Fig. 5.

Most preferred docking mode of sennoside B (in balls and sticks) on SRA domain monomer (cartoon representation). Amino acid residues involved in putative interactions are shown in green sticks representation.

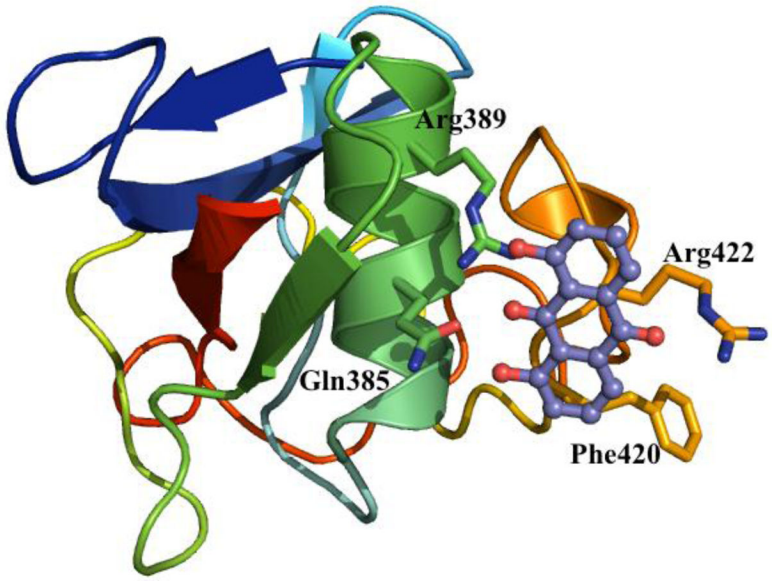

Fig. 6.

Docking modes of danthron (in balls and sticks) on Site 3 of SRA domain monomer (cartoon representation). Amino acid residues involved in putative interactions are shown in green sticks representation.

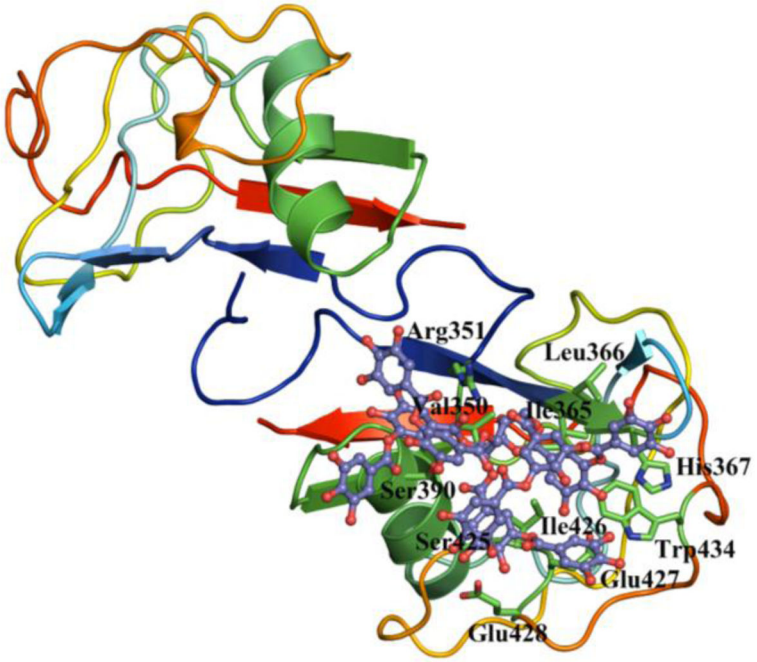

Fig. 7.

Most preferred docking mode of tannic acid (in balls and sticks) on SRA domain dimer (site 3, cartoon representation). Amino acid residues involved in putative interactions are shown in green sticks.

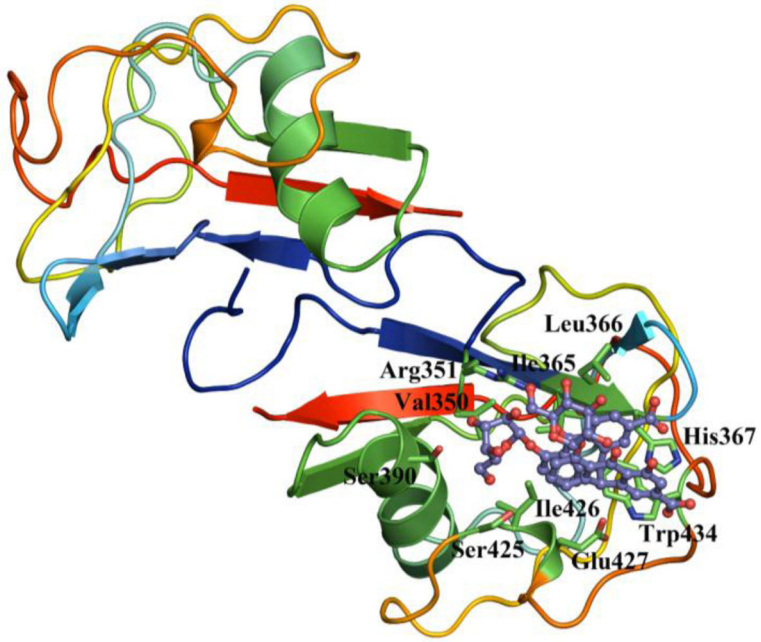

Fig. 8.

Most preferred docking mode of sennoside B (in balls and sticks) on SRA domain dimer (site 3, cartoon representation). Amino acid residues involved in putative interactions are shown in green sticks representation.

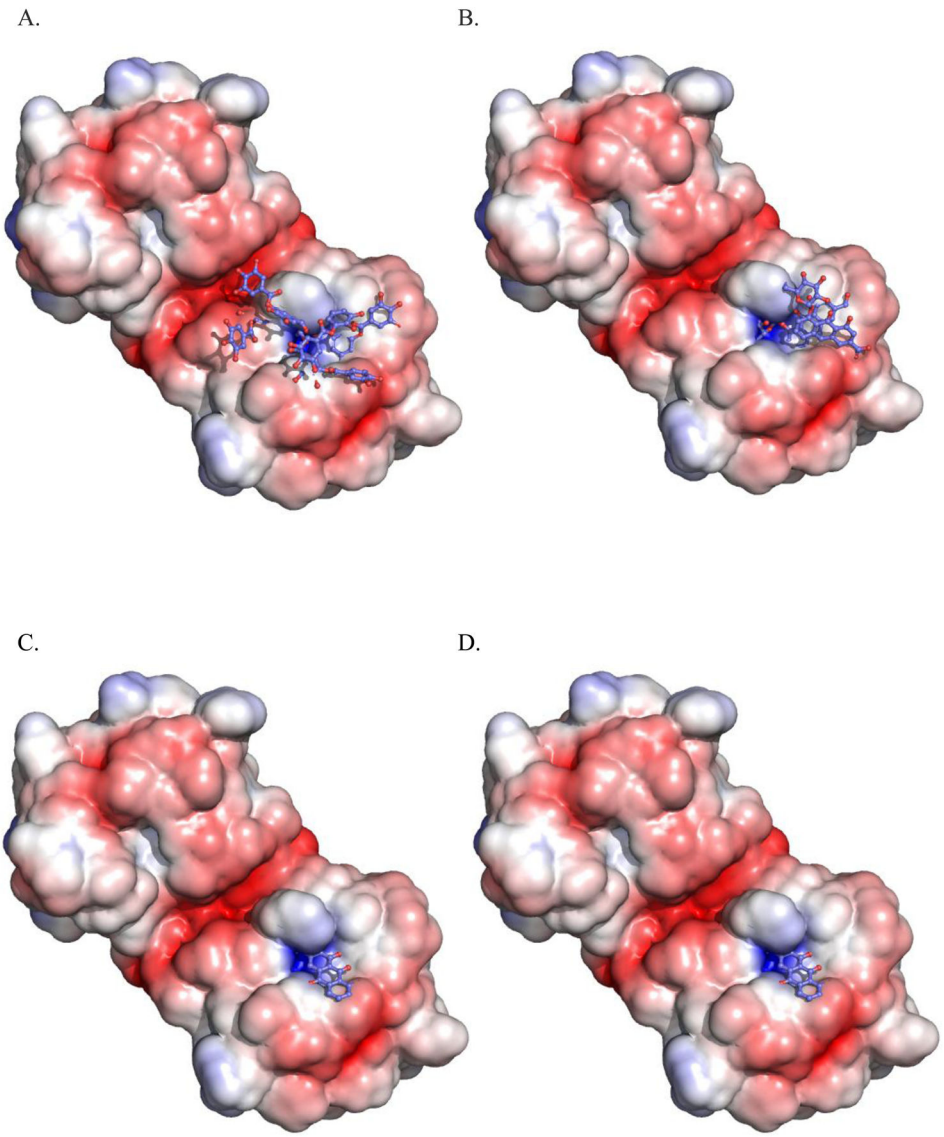

Fig. 9.

Electrostatic potential map of dimeric SRA model. Highest HINT scored docking solutions for at the most preferred docking mode for each ligand (ball and stick representations) A) Tannic acid; B) Sennoside B; C) Rhein, and D) Danthron.

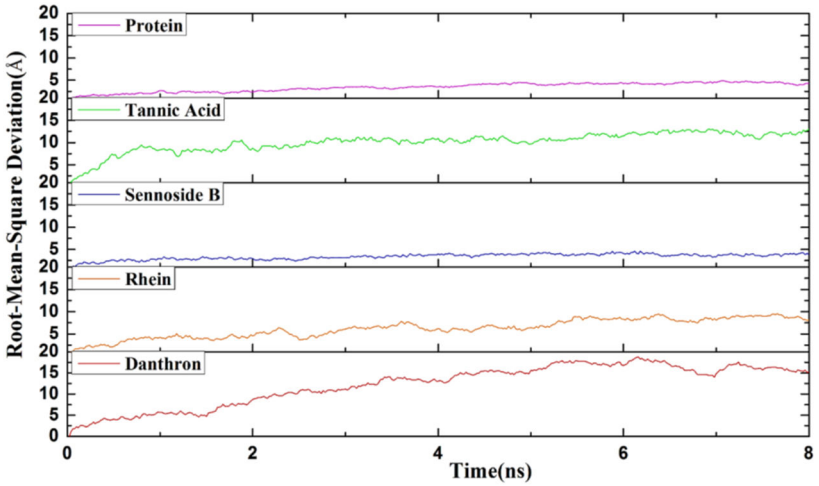

Fig. 10.

Root-mean-square-deviation (RMSD) of the protein backbone atoms of SRA dimer model and the four complexes.

A.

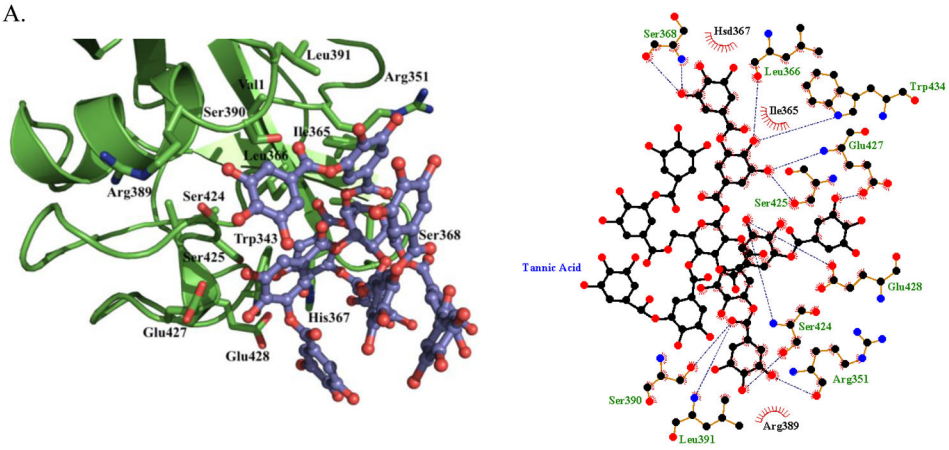

B.

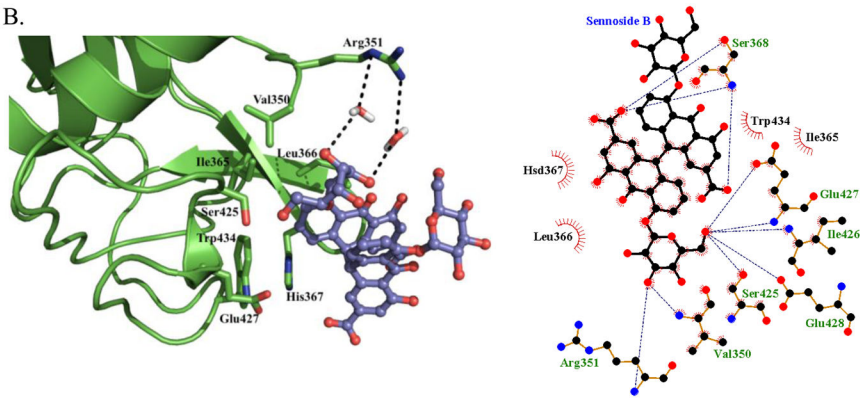

C.

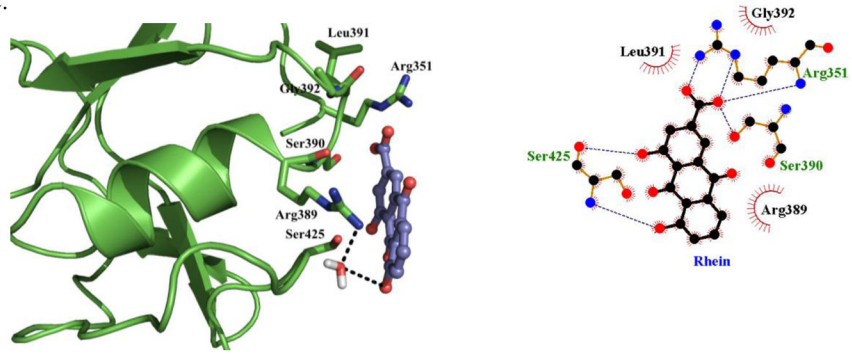

D.

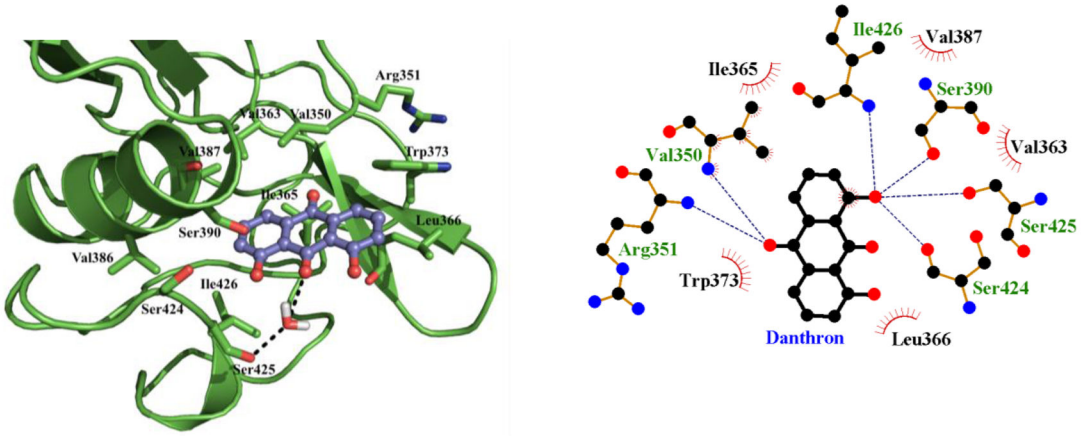

Fig. 11.

Binding pose for each ligand (ball and stick representations –left and 2D –right) after MD simulations– A) Tannic acid; B) Sennoside B; C) Rhein, and D) Danthron.

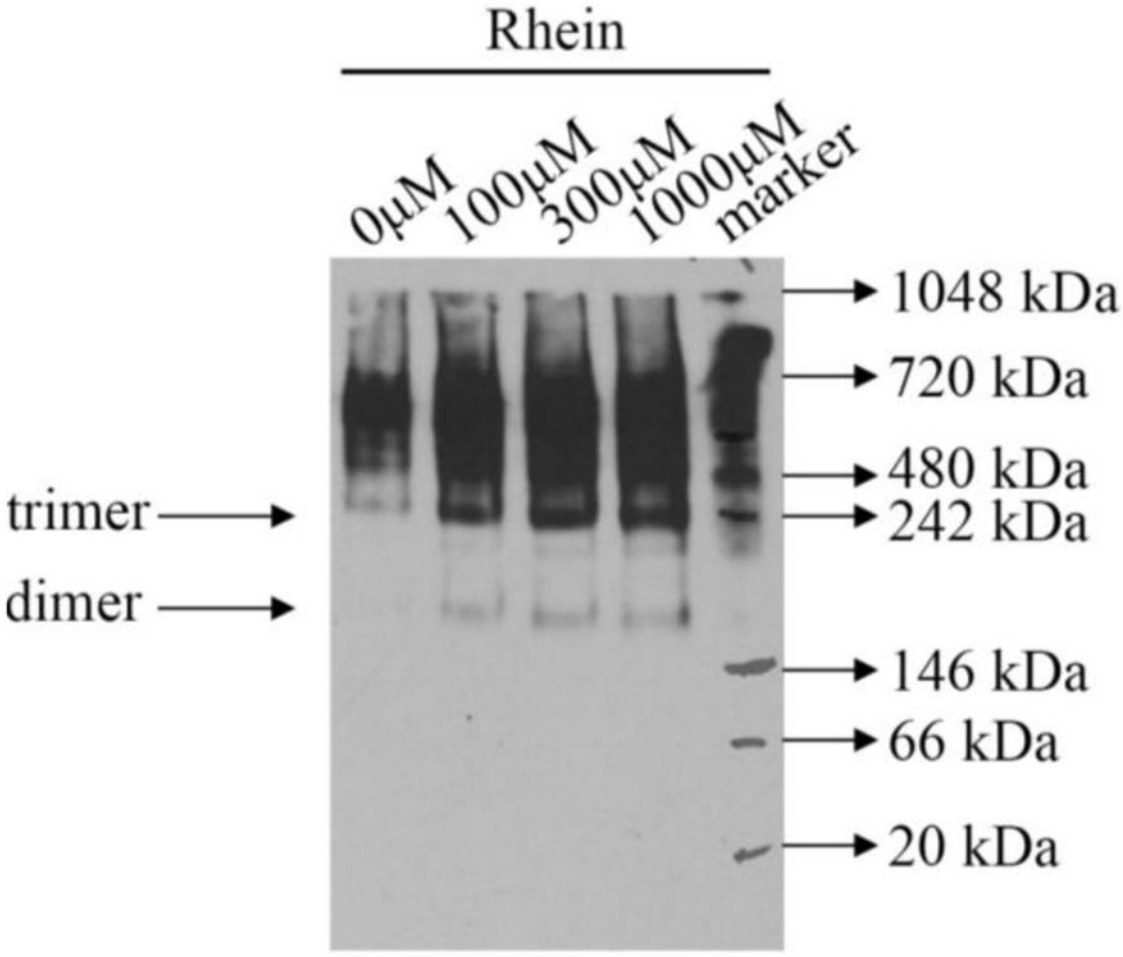

Fig. 12.

Treatment with rhein affects the oligomerization of SRA. The culture media containing secreted SRA protein was incubated with or without rhein at concentrations indicated, followed by analysis using native PAGE. Lane 1: control; lane 2: 100 μM rhein treated; lane 3: 300 μM rhein treated; lane 4: 1000 μM rhein treated; lane 5: native marker.

Table 1

Tannic acid docking sites and scoring summary (the most favored binding sites in bold/italics).

		Best HINT	Average HINT	Boltzmann average HINT
Monomer	Site 1	***2488***	***−195***	***2176***
	Site 2	***2627***	***1391***	***2318***
	Site 3	***2916***	***1468***	***2623***
	Site 4	***2656***	***1387***	***2393***
	Site 5	1727	465	1322
Dimer	Site 1	2086	−712	1869
	Site 2	1029	−1014	766
	Site 3	***4170***	***1073***	***4109***
	Site 4	2362	662	2085

Table 2

Sennoside B docking sites and scoring summary (the most favored binding site in bold/italics).

		Best HINT	Average HINT	Boltzmann average HINT
Monomer	Site 1	1025	−98	39
	Site 2	***1491***	***122***	***999***
	Site 3	761	127	428
	Site 4	769	−237	366
	Site 5	654	−41	353
Dimer	Site 1	485	−636	149
	Site 2	−666	113	−308
	Site 3	***1407***	***−215***	***1031***
	Site 4	673	−422	323

Table 3

Danthron docking sites and scoring summary (the most favored binding sites in bold/italics).

		Best HINT	Average HINT	Boltzmann average HINT
Monomer	Site 1	779	−849	168
	Site 2	478	211	265
	Site 3	***661***	***562***	***573***
	Site 4	810	169	342
	Site 5	282	55	70

Table 4

Critical amino acid residues in the docking poses for four inhibitors (the major interacting amino acid residues in bold/italics).

	Tannic Acid				**Sennoside B**	**Rhein**	**Danthron**
Monomer	**Site 1**	**Site 2**	**Site 3**	**Site 4**	**Site 2**	**Site 2**[18]	**Site 3**
	Val350, Ile365, Leu366, His367, Ser390, Leu391, Leu415, Ser425, Ile426, Glu427, Glu428, Ile431, Trp434.	Glu380, Val381, ***Arg382, Gln385, Arg389,*** Gln397, Phe420, ***Arg422,*** Glu423, Thr450, Leu451	Asp377, Arg378, Glu380, ***Arg382,*** Phe418, Phe420, ***Arg422,*** Glu423, Glu428, Arg432.	Glu360, Glu380, Val381, Gln397, Val399, His400, Lys401, His404, Phe405, Asn407, Ser442.	Glu380, Val381, ***Arg382, Gln385,*** Gln397, Phe420, Thr450.	***Arg382, Gln385, Arg389, Arg422.***	***Gln385, Arg389,*** Phe420, ***Arg422.***
Dimer	Site 3				Site 3	Site 3[18]	Site 3[19]
	Arg351, Ile365, Leu366, His367, ***Ser390,*** Leu391, ***Ser425, Ile426, Glu427,*** Glu428, Trp434.				***Val350***, ***Arg351, Ile365, Leu366,*** His367, ***Ser390, Ser425, Ile426, Glu427,*** Trp434.	***Arg351, Ile365, Leu366, Ser390, Ser425, Ile426, Glu427***, Ile431.	***Val350***, ***Ile365***, ***Leu366***, ***Ser390***, ***Ser425***, ***Ile426***.

Table 5

Critical amino acid residues involved in interactions with the four inhibitors (amino acid residues common to docking results in italics, new interacting residues after MD simulation in bold).

	Tannic Acid	Sennoside B	Rhein	Danthron
Residues	*Val350, Arg351, Ile365, Leu366, His367,* **Ser368**, **Arg389**, *Ser390,* **Leu391, Ser424**, *Ser425, Glu427, Glu428, Trp434.*	*Val350, Arg351, Ile365, Leu366, His367,* **Ser368**, *Ser425,* **Ile426**, **Glu428,** *Glu427, Trp434.*	*Arg351,* **Arg389**, *Ser390,* **Leu391**, *Ser425,* **Glu428**, **Gly392**.	*Val350, Arg351,* **Val363**, *Ile365, Leu366,* **Trp373**, **Val386**, **Val387**, *Ser390,* **Ser424**, *Ser425,* **Ile426**.